Chemical Engineering Journal 171 (2011) 674–683

Contents lists available at ScienceDirect

Chemical Engineering Journal

journal homepage: www.elsevier.com/locate/cej

Comparative study of the synthesis of silica nanoparticles in micromixer–microreactor and batch reactor systems

Laura Gutierrez[a,b], Leyre Gomez[a], Silvia Irusta[a], Manuel Arruebo[a,*], Jesus Santamaria[a,c,*]

[a] Aragon Institute of Nanoscience (INA), Edificio I+D+i, C/Mariano Esquillor s/n, University of Zaragoza, 50018 Zaragoza, Spain
[b] Institute of Research on Catalysis and Petrochemistry–INCAPE-(FIQ, UNL-CONICET), Santiago del Estero 2829, 3000 Santa Fe, Argentina
[c] Networking Research Center on Bioengineering, Biomaterials and Nanomedicine, CIBER-BBN, 50018 Zaragoza, Spain

ARTICLE INFO

Article history:
Received 23 March 2011
Received in revised form 29 April 2011
Accepted 6 May 2011

Keywords:
Micromixer
Stöber silica
Continuous synthesis
Nanoparticles
Microreactor

ABSTRACT

Two different reactors, namely a microreactor with an interdigital micromixer and a batch reactor, have been used to prepare silica nanoparticles. The effect of synthesis variables was studied, and the results are compared in terms of particle-size distribution and synthesis reproducibility for different reaction conditions. The microreactors operated with shorter nucleation times and a greater homogeneity in terms of temperature and composition. This resulted in narrower particle-size distributions and a lower polydispersity. The synthesis reproducibility and the reactant (TEOS) conversion were also higher when using micromixers compared with batch reactors for the same synthesis times. Because of these characteristics micromixer–microreactor systems appear as a promising alternative for the continuous synthesis of nanoparticles.

1. Introduction

Batch reactors still constitute the most frequently used system in the wet synthesis of nanoparticles. This is so in spite of several obvious drawbacks such as: (i) heterogeneous distribution of reactants and temperature in the reactor, (ii) insufficient mixing, (iii) variations in the physicochemical characteristics of the resulting products among different batches, (iv) inherent discontinuity, (v) difficulty of scaling-up, and (vi) frequent need for post-synthesis purification steps [1].

In order to overcome these disadvantages micro-scale reactors (i.e., micromixers, capillaries, junctions, etc.) have been used in the synthesis of nanoparticles to afford a precise control of reaction temperatures and residence times rendering nanoparticles with narrow particle-size distributions. This monomodal distribution is desirable because many physical properties of nanomaterials (e.g., optical band gaps in semiconductors, plasmon band energy in noble metals, superparamagnetism in metals and metallic oxides, or the ability to penetrate cells in biological applications) strongly depend on their size, shape and aspect ratio.

The small channel dimensions in the microreactors lead to large surface area-to-volume ratios (10,000–50,000 m^2/m^3 compared to 100 m^2/m^3 for batch reactors) and to fast heat and mass transport [1]. Other desirable characteristics refer to their inherent continuous nature and easy scale-up by replica. Because of this, microreactors have been proposed for the synthesis of nanoparticulated materials such as quantum dots [2–4], Au [5,6], TiO_2 [7], Co [8,9], Fe_3O_4 [10,11], Ag [12], $BaSO_4$ [13,14], SiO_2 [15], Cu [16], NaA zeolites [17], α-FeO(OH) (goethite) [18], LaF_3:Ce,Tb [19], etc., as well as, core/shell-based nanoparticulated materials such as Au/Ag [20], CdSe/ZnS [21,22], SiO_2/TiO_2 [23], γ-Fe_2O_3/SiO_2 [24], etc. Other reports on continuous-flow synthesis of nanoparticles are summarized elsewhere [25]. Other works [26–28] have also demonstrated the ability of microreactors to provide good control over other critical factors such as pH, crystallinity and stability against oxidation of the resulting metallic products.

There are also shortcomings of microreactors: the microfabrication techniques used in their manufacture are expensive, some of the materials used make it complicated to weld and to achieve a gas-tight sealing, the connection from the micro to the macroscale is often not straightforward, modifications in a finished microfabricated microreactor are not economically viable, plugging and fouling may occur (thus, a pre-purification, by filtration of the feed streams is usually advisable), and the stacking of several microreactors for scale-up is not trivial because of the difficulties in achieving a uniform flow split towards each microreactor from a single feed stream [29].

In this work we have selected one of the most widely used nanoparticles (silica) and a well-known synthesis process (Stöber) to compare the performance of micromixer/microreactor units against a conventional batch reactor. The comparison follows the quality of the product obtained in terms of polydispersity (related

* Corresponding authors. Tel.: +34 976 761000x5437; fax: +34 976761879.
E-mail address: arruebom@unizar.es (M. Arruebo).

1385-8947/$ – see front matter © 2011 Elsevier B.V. All rights reserved.
doi:10.1016/j.cej.2011.05.019

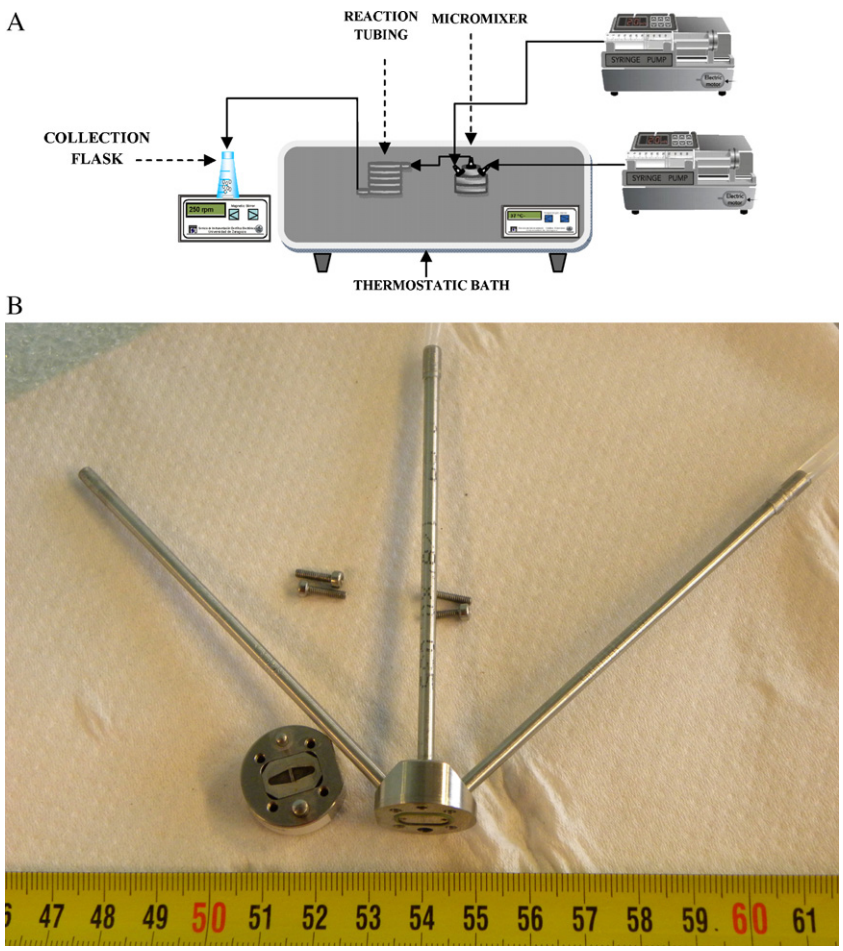

Fig. 1. (A) Experimental set up for the continuous nanoparticle synthesis. (B) Standard slit interdigital microstructured mixer used in this work.

to the width of the particle size distribution) and the synthesis reproducibility. We chose silica nanoparticles not only because of the wide ranging applications of silica nanoparticles in biomedicine (i.e., fluorescent probes for bioanalysis, drug and gene delivery vectors, in bioseparation, as drug coadjutants, etc.), in the polymer industry (as fillers to improve the mechanical properties of polymers in nanocomposites or to reduce their thermal conductivity as heat-insulation fillers; in paints, to control their rheological properties, etc.), in catalysis, adsorption storage and so on [30], but also because the Stöber synthesis [31] is perhaps the friendliest of nanoparticle fabrication processes: under batch conditions it presents good reproducibility and renders a relatively narrow nanoparticle size distribution. In addition, it takes place at low temperatures, removing the need for rapid heating or cooling of reactants. If even in this highly favorable case the advantages of a simple microreactor design could be demonstrated, it would constitute a powerful argument for making microreactors the system of choice in nanoparticle synthesis.

2. Materials and methods

Silica nanoparticles were prepared using a protocol similar to the one described by Pham et al. [32]. The synthesis was carried out at different temperatures with TEOS (tetraethyl orthosilicate, 98%, Sigma Aldrich, USA) as the silica source and ammonium hydroxide as catalyst. Two different solvents (ethanol and methanol) were employed, as they are known to give rise to different product characteristics. In order to minimize gradients in the batch reactor, batch synthesis was carried out with a reduced reaction volume (15 mL) under continuous stirring at 400 rpm, immersing the reaction vessel in a temperature controlled bath.

The microreactor system comprised a standard slit interdigital microstructured mixer from IMM (Institut für Mikrotechnik Mainz GmbH, Germany) followed by a variable length of capillary (1.3 mm internal diameter) Tygon® pipe. Continuous synthesis was carried out by feeding the reactants to the micromixer by means of infusion syringe pumps from KD Scientific Inc. (model KDS100) (Fig. 1). In the micromixer the inlet streams was divided in 16 sub-streams and recombined in order to maximize the contact area. In this way, by thinning the multilamellar flow the mixing speed increases, and the exit tube following the micromixer contains a completely mixed stream. The microreactor feed comprised two separate stock solutions, one with the TEOS and half of the corresponding solvent and the other with the ammonia (the amounts used were proportional to the ones used in the batch synthesis) and the other half of the solvent that were respectively loaded into each feeding syringe. The exit stream leaving the micromixer was allowed to react further in the 1.3 mm i.d. Tygon® capillary pipe until the particles reached the desired size. To this end, the length of the pipe was adjusted to reach the requested residence time. The microreactor (micromixer plus Tygon tubing) were immersed in a thermostatic water bath in order to control the reaction temperature (Fig. 1). The mean residence time was calculated as the ratio of the reactor volume (including the volume of the micromixer and the tubing) to the total volumetric flow rate. The exit stream was collected in a flask with an excess of solvent to assure a rapid quenching of the reaction.

The physical characterization of the resulting nanoparticles either as dry powders or as aqueous dispersions was carried out by

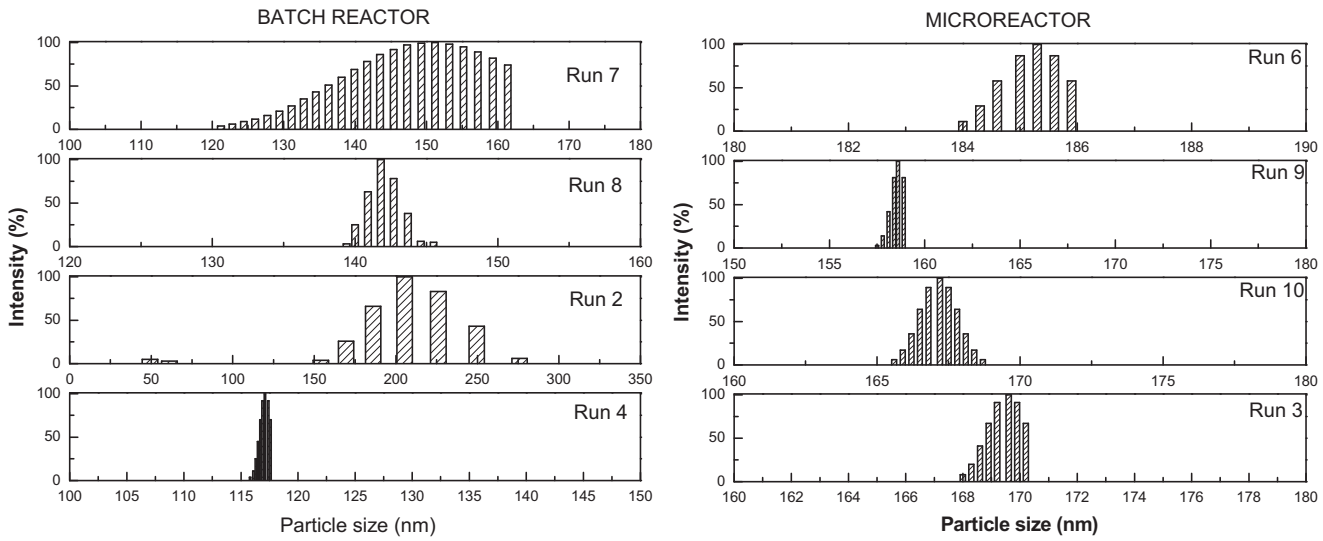

Fig. 2. Intensity particle-size distributions obtained for some of the runs depicted in Table 1 for the batch and the microreactor.

scanning electron microscopy, SEM (FEI Instruments model Inspect F) and dynamic light scattering, DLS (90 Plus, Brookhaven Instruments Corp.), respectively. FTIR, XPS and X-ray fluorescence were also used to evaluate the TEOS conversion into silica at different residence times and where possible, Si mass balances were also carried out. Fourier transform infrared (FTIR) spectroscopy of the particles was performed with a Bruker Vertex 70 FTIR spectrometer equipped with a DTGS detector and a Golden Gate diamond ATR accessory. Spectra were recorded by averaging 40 scans in the 4000–600 cm^{-1} wave number range at a resolution of 4 cm^{-1}. Data evaluation was carried out by using the OPUS software from Bruker Optics, Inc. X-ray photoelectron analysis (XPS) was performed with an Axis Ultra DLD (Kratos Tech.). The spectra were excited by the monochromatized AlKα source (1486.6 eV) run at 15 kV and 10 mA. For the individual peak regions, pass energy of 20 eV was used. Each survey spectrum was measured at 160 eV pass energy. Analyses of the peaks were performed using a weighted sum of Lorentzian and Gaussian component curves after Shirley background subtraction. The binding energies were referenced to the internal C 1s (284.9 eV) standard. X-ray fluorescence using an ADVANT'XP XRF spectrometer from Thermo Electron, Corp. was used to evaluate the total amount of silicon in the resulting dispersions.

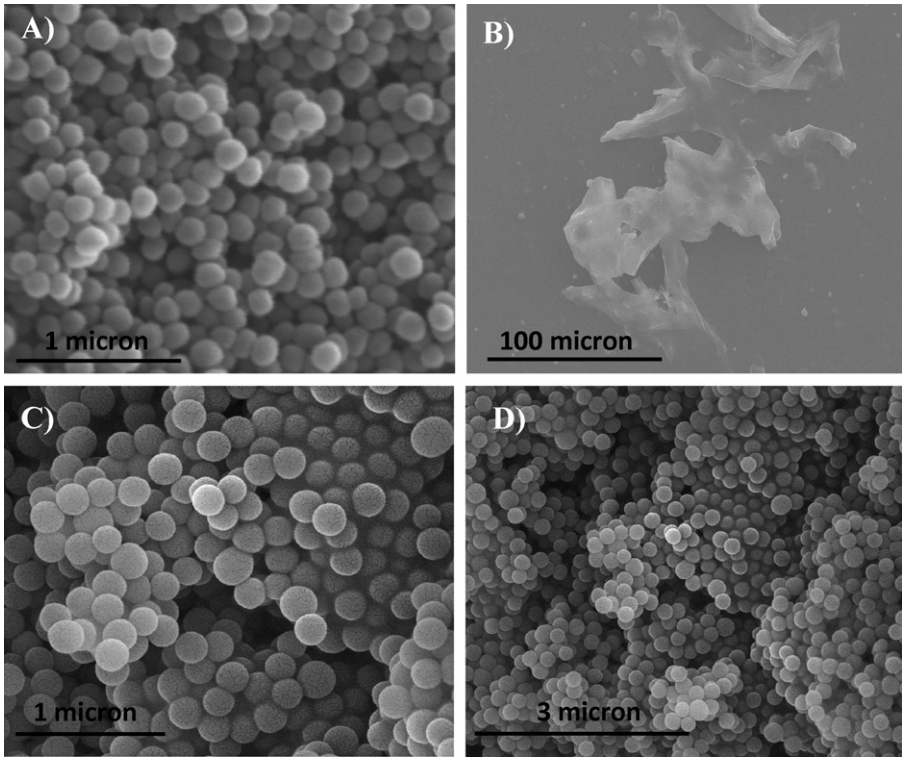

Fig. 3. SEM photographs of the resulting nanoparticles obtained with the same chemical composition (corresponding to A and B in Table 3), and for different reactor systems and residence times. (A) Batch reactor (120 min); (B) microreactor (15 min residence time); (C and D) microreactor (30 min residence time).

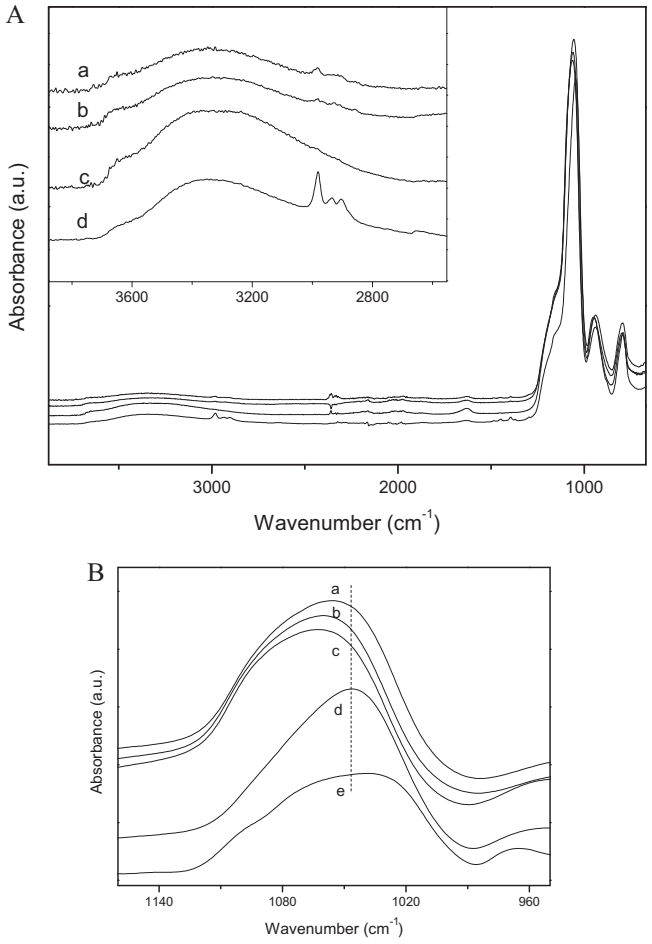

Fig. 4. (A) FTIR spectra of nanoparticles obtained in system B at different residence times: (a) 15 min, (b) 30 min and (c) 90 min and (d) nanoparticles obtained with the batch reactor after 2 h reaction, (B) Comparison of the Si–O–Si asymmetric stretching band for the prepared samples compared with (e) TEOS Si–O–Si band.

3. Results

Table 1 shows the mean hydrodynamic diameter and the polydispersity obtained for both reactors in 10 independent experiments, together with the mean values and the maximum difference

Table 1
Hydrodynamic diameters for the resulting silica nanoparticles measured as aqueous dispersions. Synthesis conditions: temperature: 40 °C, composition of the reacting mixture corresponding to system B (see Table 3).

	Microreactor		Batch	
	Hydrodynamic diameter (nm)	Polydispersity[a]	Hydrodynamic diameter (nm)	Polydispersity[a]
Run 1	185	0.005	183	0.005
Run 2	137	0.009	205	0.025
Run 3	169	0.006	204	0.012
Run 4	159	0.030	117	0.005
Run 5	194	0.021	151	0.007
Run 6	185	0.005	148	0.009
Run 7	159	0.015	148	0.025
Run 8	184	0.023	142	0.028
Run 9	157	0.008	160	0.047
Run 10	169	0.005	180	0.009
ΔD_{max}	57		88	
Mean	169.8	0.0127	163.8	0.0172
SD	17.4		28.46	

[a] Polydispersity is automatically calculated by the system software from the cumulant analysis as defined in ISO 13321:1996.

Table 2
XPS results for nanoparticles obtained in the interdigital micromixer. Composition of the reacting mixture corresponding to system B (see Table 3).

Residence time (reacting system)	Binding energy (eV)			C/Si	O/Si
	C 1s	O 1s	Si 2p		
15 min (microreactor)	284.9	532.8	103.5	1.8	3.5
30 min (microreactor)	284.9	533.1	103.9	0.4	2.8
90 min (microreactor)	284.9	532.9	103.6	0.2	2.1
120 min (batch)	284.9	532.8	103.4	1.2	3.1

in the mean diameter from any two experiments. The results clearly indicate that, while the average diameters are roughly similar (169.8 against 163.8 nm) the polydispersity is lower (about 26% lower) when using the micromechanized micromixer and the reproducibility is higher (the maximum difference between any two experiments is 35% lower and the standard deviation of the mean hydrodynamic diameter is 39% lower for the microreactor compared to the batch system). Fig. 2 shows graphically this narrower particle size distribution obtained for some of the runs described in Table 1 when using the interdigital micromixer.

Fig. 3 shows the morphology of the silica nanoparticles obtained from both reactors at different residence times using the same feed composition. Samples were collected at the exit of the microreactor at different residence times (15, 30 and 90 min) and the size of those resulting nanoparticles remained unchanged when using 30 and 90 min as residence times, indicating that, the reaction was essentially complete for residence times above 30 min. In contrast, samples collected after a residence time of 15 min still evolve, changing their morphology and size in the collection flask indicating that the reaction was not completed in the microreactor. In agreement with this, Fig. 3B shows the presence of amorphous gel-like silica without the characteristic spherical shape of finished particles (Fig. 3C).

Fig. 4 shows the FTIR spectra of SiO_2 nanoparticles synthesized at different residence times. The strong absorption bands in the 1062–1054 cm^{-1} range and the shoulders around 1159 cm^{-1} can be assigned to the stretching vibration mode of Si–O–Si bond [33]. This peak was used for the intensity normalization of spectra. The band at 794 cm^{-1} is related to Si–O–Si symmetric stretching vibration, while the signal at 940 cm^{-1} would be related to Si–OH bonds [34]. FTIR spectra of nanoparticles synthesized in the micromixer at 15 min residence times (Fig. 4A, curve a) clearly displays bands in the 3000–2800 cm^{-1} range characteristic of the C–H stretching and deformation vibrations form the ethoxy groups ($-OC_2H_5$) due to the incomplete hydrolysis of TEOS [35]. These bands are still discernible, though with some difficulties after 30 min reaction (curve b) and practically vanish (curve c) at 90 min residence time. This is in contrast with the spectra of the nanoparticles prepared in the batch reactor (curve d in Fig. 4A), where after 120 min of reaction the C–H stretching bands are still strong, suggesting a high non-reacted TEOS concentration in this material.

Fig. 4B compares the bands in the range related to Si–O–Si symmetric stretching mode. TEOS also presents a peak in this range (1038 cm^{-1}) assigned to Si–O–C vibration [36]. As the reaction proceeds, the peak shifts to higher wavenumbers, suggesting the decrease of Si–O–C bonds due to non hydrolyzed TEOS. Fig. 4B shows that the wavenumber increases in the order: curve e (TEOS) < curve d (batch reactor) < curve a (microreactor, 15 min) < curve b (microreactor, 30 min) ≈ curve c (microreactor, 90 min), which corresponds with the above discussion on the degree of completion of reaction in the batch and microreactor systems.

The FTIR results were also confirmed by XPS elemental analysis. The results are shown in Table 2 for nanoparticles prepared in the microreactor and the batch reactor, with the same feed composi-

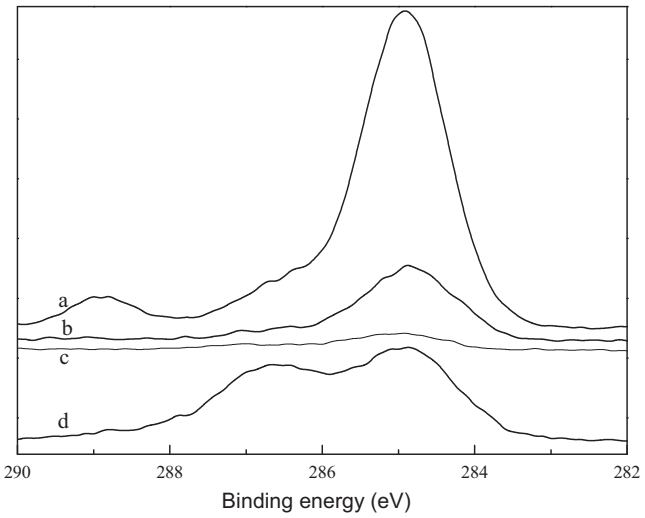

Fig. 5. Narrow scan XPS spectra of C 1s core level for nanoparticles obtained for system B in the micromixer with residence time (a) 15 min, (b) 30 min, (c) 90 min, and (d) in batch reactor after 120 min reaction.

tion (A, Table 3). The wide scan of all samples consisted of carbon (C 1s) peak at 284.9 eV along with the oxygen (O 1s around 533.0 eV) and silicon peaks (Si 2p in the 103.4–103.9 eV range). These values are typical for silicon atoms coordinated in SiO_2 [34]. Usually the C 1s peak is related to the presence of atmospheric contamination, but in these samples, according to FTIR results, it would also came from the non-reacted precursor. Fig. 5 shows the C 1s spectra obtained for all the samples, it is clearly seen that there is an important decrease in the concentration of carbon after 30 min reaction in the micromixer, and it is even lower after 90 min of reaction. On the other hand, the sample obtained in the batch reactor showed the presence of a high amount of superficial carbon that would came from remaining un-reacted TEOS. It is interesting to look at the O/Si ratio for the nanoparticles obtained in the batch reactor, which shows a value close to that of TEOS molecule (O/Si = 4) while the nanoparticles obtained in the interdigital micromixer at 90 min. residence time have a O/Si ratio close to that of the SiO_2 molecule (O/Si = 2).

Finally, X-ray fluorescence was also used to determine the amount of Si remaining in the products stream. To this end, the reacted solution was analyzed after separating by filtration (using a filter with a 5 nm nominal cut-off size) the resulting silica nanoparticles. For the batch reactor the results show that after 2 h of synthesis some silicon (0.125 wt.%) is still present in the supernatant and, therefore, it remained unconverted. On the contrary, in the microreactor the analysis for the collected supernatants of the resulting synthesis products did not show any silicon (values below the detection limit of the equipment). Summarizing, the mass balance, X-ray fluorescence, FTIR and XPS results indicate that in the microreactor system used all the TEOS is converted between 30 and 90 min. In contrast, in the batch reactor the amount of unconverted TEOS after 2 h of reaction is clearly higher than for the microreactor after only 30 min of reaction time.

Table 3 shows the main experimental conditions used in both kinds of reactors. For the experiments in this table, the amount of silica precursor, water content and catalyst in the precursor solution were varied, while the reaction temperature was kept constant (40 °C). The influence of temperature is presented in Fig. 6 where the evolution of the average particle size with synthesis time at different temperatures is presented for systems A and B (no water added other than that in the ammonia solution). For the batch system, it can be seen that the particle size in some cases continues to increase well after 120 min

Table 3
Main experimental conditions and characteristics of the particles obtained in the different synthesis experiments.

System	Reactor	TEOS/NH_4OH (molar ratio)	TEOS/H_2O (molar ratio)	TEOS/ROH (molar ratio)	NH_4OH (mol/L)	H_2O (mol/L)	TEOS (mol/L)	Average particle size[b] (nm) (residence time)	Polydispersity index (PDI)
A	Microreactor	1/11	1/138	1/132 ROH = ethanol	1.12	8.4	0.102	298 (90 min)	0.036
								276 (30 min)	0.011
	Batch							274	0.040
B	Microreactor[a]		1/24		1.26	2.78	0.166	197	0.018
								170[c]	0.012[c]
	Batch[a]							195	0.018
								164[c]	0.017[c]
C	Microreactor		1/138	1/132 ROH = methanol	1.12	8.4	0.102	65.6	0.02
	Batch							57.6	0.043
D	Microreactor	1/22	1/162	1/265 R = EtOH	1.14	8.5	0.052	247 (30 min)	0.005

[a] No water is added. The only water used is the one provided by the ammonia solution.
[b] Synthesis temperature = 40 °C. Intensity-averaged particle hydrodynamic diameter.
In all cases the microreactor was operated with a total feed volume of 9.4 mL/h, corresponding to a Reynolds number Re = 1.54.
The residence time for the batch system was 120 min in all cases.
[c] Averaged data from Table 1.

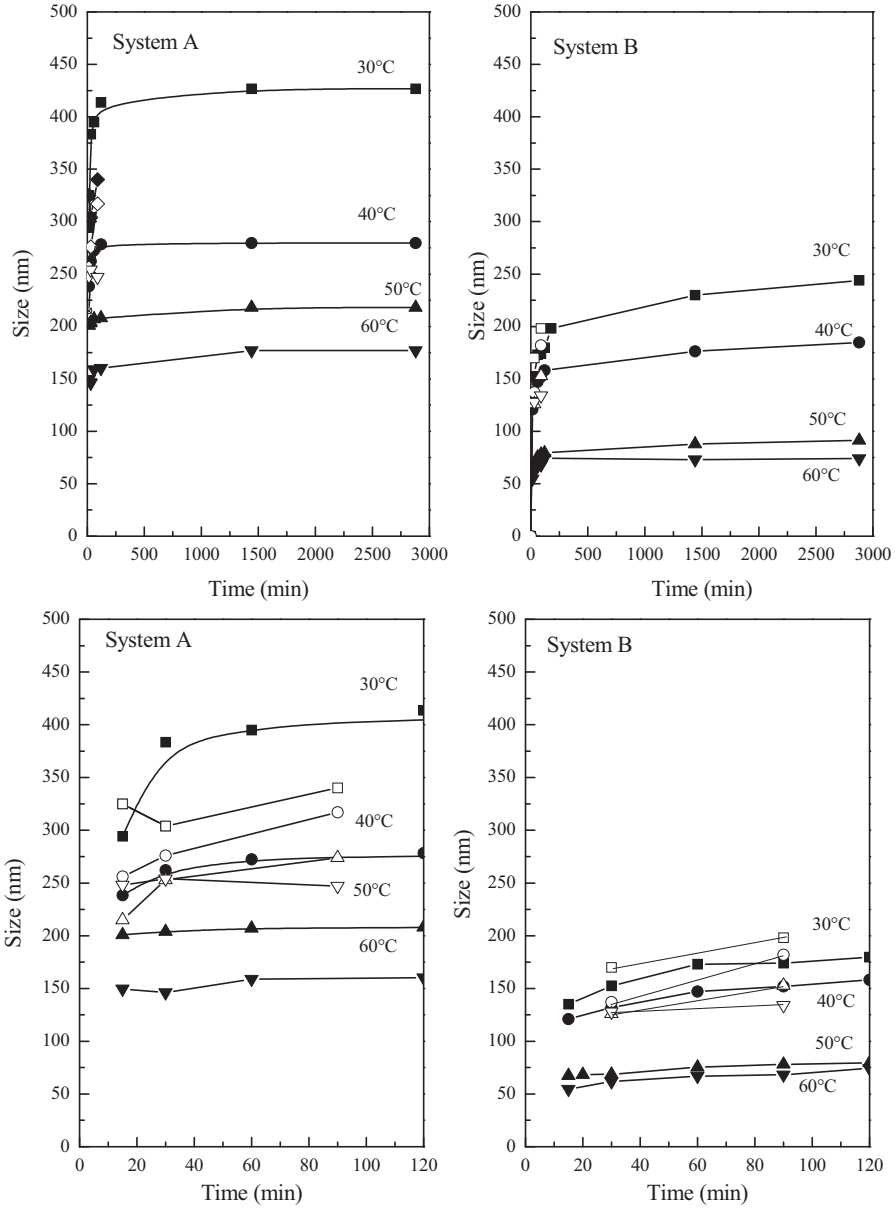

Fig. 6. Temperature and water addition influence in the size of the resulting nanoparticles when using: batch reactor (closed symbols); microreactor (open symbols). ■, □: 30 °C, ●, ○: 40 °C, ▲, △: 50 °C, ▼, ▽: 60 °C. Bottom: zoom in the first 2 h of reaction. Experimental conditions for System A and B are defined in Table 3.

of reaction time. It can also be observed that the particle size decreases as the reaction temperature increases and, for the same temperature, precursor gels with higher water content produce nanoparticles with larger sizes. Also, in the batch system the period required to reach a stable particle size shortens for gels richer in water.

Fig. 7 shows the variation of the average particle size as a function of temperature for both reacting systems and for different feed compositions. In the batch reactor the decrease of temperature with particle size is much steeper than for the micromixer. For instance, for composition A, an increase of temperature from 30 to 60 °C decreases the average particle size from 425 to 180 nm, a decrease of roughly 8 nm per °C. For the same composition in the microreactor at 90 min residence time the average size goes from 335 to 255 nm, a slope of less than 3 nm/°C. This difference in temperature sensitivity may be important when discussing the different behavior of the microreactor and the batch reactor. We measured the time necessary to reach the reaction temperature and found that in the batch reactor 4 min were necessary to reach 40 °C (and longer times for higher temperatures) when the reactants were fed at room temperature (24 °C) whereas the high surface area to volume in the microreactor allowed the reaction temperature to be reached almost instantaneously.

The effect of introducing methanol instead of ethanol as a solvent is depicted in Fig. 8. With methanol the nanoparticle size decreases compared to the results obtained when using ethanol as solvent. With both alcohols, the particle size decreases for higher temperatures, but the slope is considerably smaller than for ethanol. It is also interesting to note that when methanol is used as solvent the average particle size at a given temperature is smaller for the batch reactor.

4. Discussion

Silica formation involves two separate steps: hydrolysis of TEOS and condensation. Hydrolysis is a slow reaction, even when an

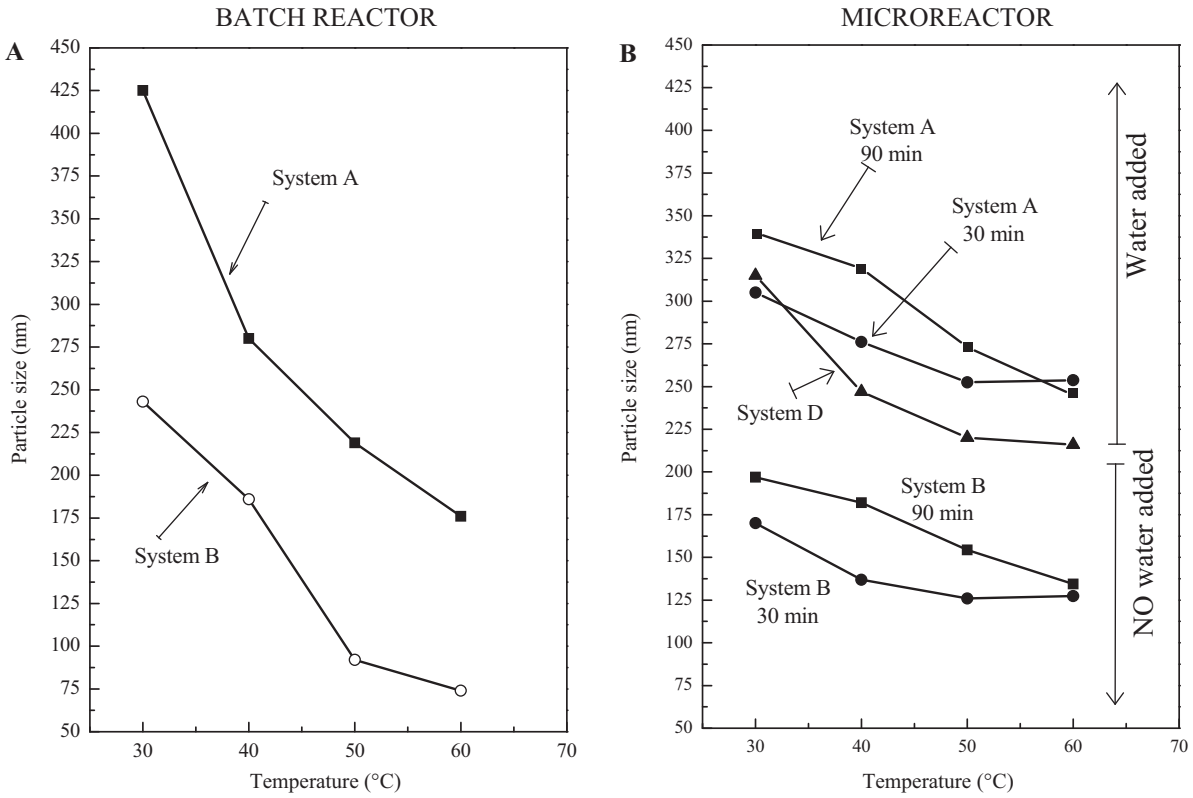

Fig. 7. Variation of particle size with temperature for the different experimental conditions in the (A) batch and (B) microreactor systems. *Note:* to ensure total conversion in the batch reactor the results shown correspond to 48 h of reaction time.

acid or a base is used as a catalyst, and higher ammonia and water concentrations can be used to accelerate the process [37]. TEOS is hydrolyzed producing siloxane molecules and ethanol. Those siloxane molecules condense with TEOS molecules releasing ethanol (alcoholic condensation) or with themselves releasing water (aqueous condensation). All the chemical reactions involved are as follows [38]:

$$Si(OR)_{4-x} + xH_2O \rightarrow (OH)_xSi(OR)_{4-x} + xROH\,(\text{TEOS hydrolysis}) \quad (1)$$

$$(OH)_ySi(OR)_{4-y} + yNH_3 \rightarrow (OR)_{4-y}Si(O^-)_y + yNH_4{}^+ \times (\text{ionization of hydrolyzed monomers}) \quad (2)$$

$$Si(OR)_4 + zR'OH \Leftrightarrow (OR')_zSi(OR)_{4-z} + zROH\,(\text{ester hydrolysis}) \quad (3)$$

$$Si(OR)_4 + (OH)Si(OR)_3 \Leftrightarrow (OR)_3Si{-}O{-}Si(OR)_3 + ROH\,(\text{alcohol condensation}) \quad (4)$$

$$(OR)_3Si(OH) + (OH)Si(OR)_3 \Leftrightarrow (OR)_3Si{-}O{-}Si(OR)_3 + H_2O\,(\text{water condensation}) \quad (5)$$

An overall mass balance indicates that the concentration of H_2O has to be twice that of TEOS to completely exhaust the silica pre-

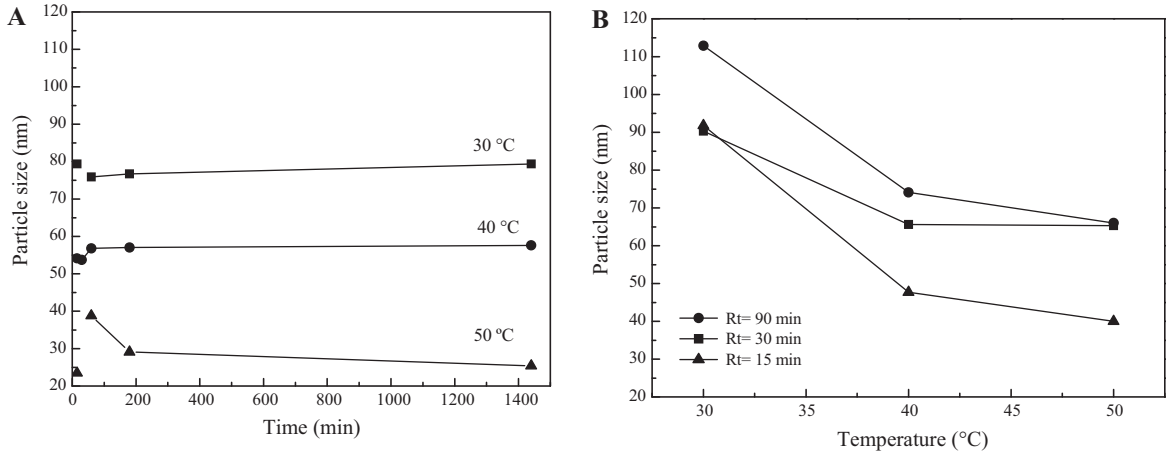

Fig. 8. Variation of particle size with time at different temperatures, for syntheses carried out using methanol instead of ethanol as the alcohol (composition C in Table 3). (A) Batch reactor and (B) microreactor.

cursor. In our case for all the systems tested water was in excess to allow the complete conversion of TEOS.

The changes in particle size with water concentration, temperature and solvent follow the expected trends. Thus other authors have already reported a larger particle size when adding water to the reactant mixture in semicontinuous synthesis processes [37]. They attributed this increase to the higher probability of the particle nuclei to agglomerate by hydrogen bonding when water is used in excess [37]. Similarly, the smaller particle size obtained when increasing the synthesis temperature is also attributed to a faster nucleation rate according to the kinetics of homogeneous nucleation in liquid phases [37]. In this way, more nuclei for the same amount of nutrients lead to a smaller mean particle size. Also, the differences observed when using methanol or ethanol as solvents has been reported by other groups [39,40]. Methanol leads to smaller nanoparticles than ethanol for the same reactant composition. Also the size of the primary particles is twice as large in ethanol as in methanol [40]. The differences are attributed to the faster hydrolysis of TEOS in methanol compared to ethanol and to the smaller size of the primary particles in methanol than in ethanol. The size dependence has been largely correlated to the decrease in the polarity of the solvents. Therefore, the general behavior with regards to the influence of temperature and water concentration in the mean nanoparticle size is in general agreement with previous results in the literature. However, the differences obtained between the batch reactor and the microreactor are significant, and more difficult to explain.

The reactions (1)–(5) given above have different kinetics, i.e. different activation energies and dependence on the concentrations of reactants. This means that small differences of temperature and/or concentration in a chemical reactor can favour one reaction at the expense of another, affecting the product characteristics (particle size distribution in this case). The general result of increased heterogeneity in the reactor volume will be a higher polydispersity of the particle size distribution. Despite the many advantages already mentioned for silica synthesis by means of the Stöber method [31] it has proven hard to achieve silica nanoparticles with polydispersity lower than 4–5% when the target size is below ca. 120 nm [41]. Usually, short-chain alcohols help to achieve particle distributions with lower polydispersity and they are therefore commonly used. Reproducibility between batches is also difficult to achieve, being affected by similar factors. Wang et al. [42] synthesized colloidal silica in presence of anionic surfactants and estimated average particle size and size distribution from different batches to be within ±10–30% being this polydispersity dependent on the different surfactant used. Khan et al. [15] compared the standard deviation (expressed as a percentage of the mean diameter) for silica nanoparticles produced in a batch reactor and in a microfluidic microreactor fabricated in poly(dimethylsiloxane) (PDMS) by using standard soft-lithographic techniques. The narrowest standard deviation was obtained with the microfluidic reactor only when segmented flow (introduction of slugs of an inert gas or a fluid to create a compartmentalization in the mixing streams) was used. The standard deviation obtained for the batch reactor was narrower than the one obtained with the microfluidic reactor when segmented flow was not used. This was attributed to the axial dispersion present in the microreactor. Nozawa et al. [43] demonstrated that the polydispersity of Stöber silica particles increased when the rate of addition of TEOS and ethanol increased in a semibatch process composed of a syringe pump feeding a constant flow rate over a flask containing ammonia and ethanol at room temperature. A fast addition of the silica source led to a heterogeneous distribution in the reacting environment.

In this work, the main findings are: (i) in the microreactor the reaction proceeds faster than in the batch reactor; (ii) the product size distribution for a given synthesis is narrower and the reproducibility between synthesis is higher for the microreactor and (iii) for the same temperature and feed composition, the batch reactor consistently gives rise to a somewhat lower average particle size.

To explain the differences observed between the results obtained in the microreactor and in the batch reactor both the reaction kinetics and the intrinsic characteristics of the reactors have to be taken into account. Because of its design, where the feed is divided into 16 sub-streams which are then recombined, mixing is extremely effective in the micromixer and homogeneity of the reactant mixture is achieved almost instantaneously. However, even though mixing in the batch system may be less effective, due to its small volume (15 mL) it seems unlikely that large composition heterogeneities can be generated. Also, it has been demonstrated that in the semibatch synthesis of Stöber silica nanoparticles the average particle size is independent of the stirring speed because when using classical stirring velocities particle growth is dominated by diffusion and hydrodynamic effects can be discarded [43]. This means that the differences between both reactors cannot be attributed exclusively to differences in composition due to inefficient initial mixing.

Two other factors that may contribute to the differences observed are solvent evaporation and temperature inhomogeneities in the batch reactor. Regarding the first, it should be noted that in the microreactor evaporation of the solvent (ethanol or methanol) is hindered or completely suppressed. However in the batch reactor solvents can evaporate, especially at higher reaction temperatures. Solvent evaporation in this case would create two types of local inhomogeneity near the solvent surface: on the one hand, the concentration of reactants in the vicinity of the surface would increase due to evaporation; on the other, evaporative cooling would cause a local reduction of temperature near the surface. In addition, in spite of the small size used for the batch reactor its surface to volume ratio is considerably smaller than for the microreactor (2.6 vs. 0.77 m^{-1} R_t = 1 h) meaning that (independently of the already noted evaporative cooling near the surface) the development of inner temperature gradients is more likely in the batch reactor.

The classical monomer-addition model proposed by LaMer and Dinegar [44] is useful here, as it describes a self-nucleation model of particle production. The first stage is the induction period, in which growth units of the solid are generated. The concentration in the surrounding solution builds up until a critical value of supersaturation is reached, at which point supersaturation is relieved through the formation of particle nuclei. Short nucleation periods occur when supersaturation is quickly relieved below the critical value, and further nucleation is prevented. This scenario leads to a narrow particle size distribution, since all nuclei grow simultaneously, incorporating material from the solution (hydrolyzed monomers in the case of silica) to the particle surface until the equilibrium solubility is reached and particle growth stops. On the contrary, in a prolonged nucleation nuclei are formed and start growing throughout an extended period, and a wide distribution of particle sizes results.

In the microreactor near-instantaneous mixing and a fast heating are expected to produce a short nucleation period, preventing further nucleation and leading to a narrow particle size distribution and to a faster completion of the reaction; On the other hand in the batch reactor longer heating times (several minutes required to reach the desired reaction temperature) and a poorer mixing are likely to result in the production of particle nuclei over longer periods of time, yielding nanoparticles with broader particle-size distributions. The size dispersion would be further enhanced by inhomogeneities in the reaction rate caused by local inhomogeneities that are more likely in the batch reactor, as discussed above. Since these inhomogeneities are difficult to control, reproducibility between reaction runs would be expected to be higher

for the microreactor. Finally, a longer nucleation period in the batch reactor would result in a larger number of nuclei, and therefore in a smaller average particle size compared to the microreactor for a given set of conditions. All of these predictions are in agreement with the results obtained in this work.

The results obtained show that the microreactor affords a better control of particle size (narrower particle size distribution) and a better reproducibility compared to the batch reactor, even for a process, like the Stöber synthesis, that is often quoted as "one of the easiest to control nanoparticle preparation procedures". This, together with the inherent advantages of continuous processes against batch operations should provide a definitive advantage in the scaling up of nanoparticle production. In fact, the superior performance of micromixers/microreactors has also been reported for the synthesis of other inorganic nanoparticulated systems. For instance, Titanium oxide nanorods were synthesized by Cottam et al. [45] in microreactors and batch reactors. They observed that the reaction rate was faster in the microreactor, with anatase TiO_2 nanorods formed in 10 min compared to over 90 min in the batch system. Edel et al. [46] demonstrated an increased monodispersity for the CdS nanoparticles synthesized by using a glass/silicon micromixer compared with the nanoparticles obtained in the batch reactor. The same observation was described by Shalom et al. [47] in the synthesis of Au nanoparticles using an interdigital micromixer and by Song et al. [48] in the synthesis of Pd nanoparticles using a continuous flow polymeric microreactor.

Additional advantages are related to the possibility of integrating completely automated systems for the synthesis of nanoparticles. In this way, Lee et al. [49] developed an automated system for the synthesis of magnetic nanoparticles capable of transporting, mixing and controlling reactions on a single chip and again the particle-size distribution obtained for the resulting nanoparticles was narrower than for those obtained in a large-scale system. Similarly, Toyota et al. [50] have also developed several microreactors combined with an on-line detector as a combinatorial synthesis system to optimize nanoparticle synthesis.

5. Conclusions

Micromixer microreactor systems produced narrower particle-size distributions compared to batch reactors in the Stöber synthesis of silica nanoparticles using the same reactant compositions and experimental conditions. The use of microreactors led to lower polydispersity, higher inter-run reproducibility and lower synthesis times, compared to the batch system. These results can be explained on the basis of a better mixing and a higher surface to volume ratio in the microreactor system used, leading to shorter nucleation times and to a higher homogeneity (composition, temperature) in the reaction mixture. Considering that an accurate control of particle size is essential since nanoparticles show size-dependent properties, and the need for production scale up given the increasing demand of nanoparticulated materials, micromixer/microreactors provide an excellent tool for the synthesis of nanoparticles.

Acknowledgments

M.A. acknowledges the support from the 2006 *Ramón y Cajal* program (order ECI/158/2005). Financial support from the CONICET (Argentina) and from MICINN is gratefully acknowledged.

References

[1] C.H. Chang, B.K. Paul, V.T. Remcho, S. Atre, J.E. Hutchison, Synthesis and post-processing of nanomaterials using microreaction technology, J. Nanopart. Res. 10 (2008) 965–980.
[2] B.K.H. Yen, A. Gunther, M.A. Schmidt, K.F. Jensen, M.G. Bawendi, A microfabricated gas-liquid segmented flow reactor for high-temperature synthesis: the case of CdSe quantum dots, Angew. Chem. Int. Ed. 44 (2005) 5447–5451.
[3] L.H. Hung, K.M. Choi, W.Y. Tseng, Y.C. Tan, K.J. Shea, A.P. Lee, Alternating droplet generation and controlled dynamic droplet fusion in microfluidic device for CdS nanoparticle synthesis, Lab Chip 6 (2006) 174–178.
[4] E.M. Chan, A.P. Alivasatos, R.A. Mathies, High-temperature microfluidic synthesis of CdSe nanocrystals in nanoliter droplets, JACS 127 (2005) 13854–13861.
[5] H. Tsunoyama, N. Ichikuni, T. Tsukuda, Microfluidic synthesis and catalytic application of PVP-stabilized, similar to 1 nm gold clusters, Langmuir 24 (2008) 11327–11330.
[6] J. Wagner, J.M. Ko1hler, Continuous synthesis of gold nanoparticles in a microreactor, Nano Lett. 5 (2005) 685–691.
[7] K.Y. Park, M. Ullmann, Y.J. Suh, S.K. Friedlander, Nanoparticle microreactor: application to synthesis of titania by thermal decomposition of titanium tetraisopropoxide, J. Nanopart. Res. 3 (2001) 309–319.
[8] Y.J. Song, L.L. Henry, W.T. Yang, Stable amorphous cobalt nanoparticles formed by an in situ rapidly cooling microfluidic process, Langmuir 25 (2009) 10209–10217.
[9] Y.J. Song, H. Modrow, L.L. Henry, C.K. Saw, E.E. Doomes, V. Palshin, J. Hormes, C. Kumar, Microfluidic synthesis of cobalt nanoparticles, Chem. Commun. 1 (8) (2006) 2817–2827.
[10] K. Sue, H. Hattori, T. Sato, T. Komoriya, A. Kawai-Nakamura, S. Tanaka, T. Hiaki, S. Kawasaki, Y. Takebayashi, S. Yoda, T. Furuya, Super-rapid hydrothermal synthesis of highly crystalline and water-soluble magnetite nanoparticles using a microreactor, Chem. Lett. 3 (8) (2009) 792–793.
[11] A.A. Hassan, O. Sandre, V. Cabuil, P. Tabeling, Synthesis of iron oxide nanoparticles in a microfluidic device: preliminary results in a coaxial flow millichannel, Chem. Commun. 178 (2008) 3–1785.
[12] J.M. Kohler, L. Abahmane, J. Wagner, J. Albert, G. Mayer, Preparation of metal nanoparticles with varied composition for catalytical applications in microreactors, Chem. Eng. Sci. 6 (3) (2008) 5048–5055.
[13] S. Li, J. Xu, Y. Wang, G. Luo, Controllable preparation of nanoparticles by drops and plugs flow in a microchannel device, Langmuir 24 (2008) 4194–4199.
[14] Y. Ying, G. Chen, Y. Zhao, S. Li, Q. Yuan, A high throughput methodology for continuous preparation of monodispersed nanocrystals in microfluidic reactors, Chem. Eng. J. 13 (5) (2008) 209–215.
[15] S.A. Khan, A. Günther, M.A. Schmidt, K.F. Jensen, Microfluidic synthesis of colloidal silica, Langmuir 20 (2004) 8604–8611.
[16] Y.J. Song Y.J., E.E. Doomes, J. Prindle, R. Tittsworth, J. Hormes, C. Kumar, Investigations into sulfobetaine-stabilized Cu nanoparticle formation: toward development of a microfluidic synthesis, J. Phys. Chem. B 109 (2005) 9330–9338.
[17] J.X. Ju, C.F. Zeng, L.X. Zhang, N.P. Xu, Continuous synthesis of zeolite NaA in a microchannel reactor, Chem. Eng. J. 1 (3) (2006) 115–121.
[18] A.A. Hassan, O. Sandre, S. Neveu, V. Cabuil, Synthesis of goethite by separation of the nucleation and growth processes of ferrihydrite nanoparticles using microfluidics, Angew. Chem. 48 (2009) 2342–2345.
[19] X.X. Zhu, Q.H. Zhang, Y.G. Li, H.Z. Wang, Redispersible and water-soluble LaF_3:Ce,Tb nanocrystals via a microfluidic reactor with temperature steps, J. Mater. Chem. 18 (2008) 5060–5062.
[20] J.M. Kohler, H. Romanus, U. Hubner, J. Wagner, Formation of star-like and core–shell AuAg nanoparticles during two- and three-step preparation in batch and in microfluidic systems, J. Nanomater. 2007 (2007) 98134.
[21] H.Z. Wang, X.Y. Li, M. Uehara, Y. Yamaguchi, H. Nakamura, M.P. Miyazaki, H. Shimizu, H. Maeda, Continuous synthesis of CdSe–ZnS composite nanoparticles in a microfluidic reactor, Chem. Commun. 4 (2004) 8–49.
[22] Ziegler F J., A. Merkulov, M. Grabolle, U. Resch-Genger, T. Nann, High-quality ZnS shells for CdSe nanoparticles: rapid microwave synthesis, Langmuir 23 (2007) 7751–7759.
[23] S.A. Khan, K.F. Jensen, Microfluidic synthesis of titania shells on colloidal silica, Adv. Mater. 1 (9) (2007) 2556–2559.
[24] A. Hassan, R. Bazzi, V. Cabuil, Multistep continuous-flow microsynthesis of magnetic and fluorescent gamma-Fe_2O_3@SiO_2 core/shell nanoparticles, Angew. Chem. Int. Ed. 4 (8) (2009) 7180–7183.
[25] D.V. Ravi Kumar, M. Kasture, A.A. Prabhune, C.V. Ramana, B.L.V. Prasad, A.A. Kulkarni, Continuous flow synthesis of functionalized silver nanoparticles using bifunctional biosurfactants, Green Chem. 1 (2) (2010) 609–615.
[26] C.R. Cabrera, B. Finlayson, P. Yager, Formation of natural pH gradients in a microfluidic device under flow conditions: model and experimental validation, Anal. Chem. 73 (2001) 658–666.
[27] S. Kawasaki, Y. Xiuyi, K. Sue, Y. Hakuta, A. Suzuki, K. Arai, Continuous supercritical hydrothermal synthesis of controlled size and highly crystalline anatase TiO_2 nanoparticles, J. Supercrit. Fluids 50 (2009) 276–282.
[28] Y. Song, E.E. Doomes, J. Prindle, R. Tittsworth, J. Hormes, C.S.S.R. Kumar, Investigation into sulfobetaine-stabilized Cu nanoparticle formation: toward development of a microfluidic synthesis, J. Phys. Chem. B 109 (2005) 9330–9338.
[29] Y. Song, J. Hormes, C. Kumar, Microfluidic synthesis of nanomaterials, Small 4 (2008) 698–711.
[30] L. Wang, W. Zhao, W. Tan, Bioconjugated silica nanoparticles: development and applications, Nano Res. 1 (2008) 99–115.
[31] W. Stöber, A. Fink, E. Bohn, Controlled growth of monodisperse silica spheres in micron size range, J. Colloid Interface Sci. 26 (1968) 62–66.

[32] T. Pham, J.B. Jackson, N.J. Halas, T.R. Lee, Preparation and characterization of gold nanoshells coated with self-assembled monolayers, Langmuir 18 (2002) 4915–4920.
[33] B. Zhou, Z. Liu, X. Wang, Y. Sui, X. Huang, Z. Lü, W. Su, Effect of SiO_2 coating on the magnetic properties of Ni–Zn ferrite, Physica B 405 (2010) 374–378.
[34] N. Moussaif, S. Irusta, C. Yagüe, M. Arruebo, J. Meier, C. Crespo, M.A. Jimenez, J. Santamaría, Mechanically reinforced biodegradable nanocomposites. A facile synthesis based on PEGylate silica nanoparticles, Polymer 51 (2010) 6132–6139.
[35] E. Juncal, J.C. Echeverría, M. Laguna, J.J. Garrido, Silica xerogels of tailored porosity as support matrix for optical chemical sensors. Simultaneous effect of pH, ethanol:TEOS and water:TEOS molar ratios, and synthesis temperature on gelation time, and textural and structural properties, J. Non-Cryst. Solids 353 (2007) 286–294.
[36] N. Primeau, C. Vautey, M. Langlet, The effect of thermal annealing on aerosol-gel deposited SiO_2 films: a FTIR deconvolution study, Thin Solid Films 310 (1997) 47–56.
[37] S.K. Park, K.D. Kim, H.T. Kim, Preparation of silica nanoparticles: determination of the optimal synthesis conditions for small and uniform particles, Colloids Surf. A: Physicochem. Eng. Aspects 197 (2002) 7–17.
[38] D.L. Green, S. Jayasundara, Y.F. Lam, M.T. Harris, Chemical reaction kinetics leading to the first Stober silica nanoparticles. NMR and SAXS investigation, J. Non-Cryst. Solids 315 (2003) 166–179.
[39] M.T. Harris, C.H. Byers, R.R. Brunson, The base-catalyzed hydrolysis and condensation reactions of dilute and concentrated TEOS solutions, J. Non-Cryst. Solids 121 (1990) 397–403.
[40] D.L. Green, J.S. Lin, Y.-F. Lam, M.Z.C. Hu, D.W. Schaefer, M.T. Harris, Size, volume fraction, and nucleation of Stober silica nanoparticles, J. Colloid Interface Sci. 266 (2003) 346–351.
[41] J. Guo, X. Liu, Y. Cheng, Y. Li, G. Xu, P. Cui, Size-controllable synthesis of monodispersed colloidal silica nanoparticles via hydrolysis of elemental silicon, J. Colloid Interface Sci. 326 (2008) 138–142.
[42] W. Wang, B. Gua, L. Liang, Effect of anionic surfactants on synthesis and self-assembly of silica colloidal nanoparticles, J. Colloid Interface Sci. 313 (2007) 169–173.
[43] K. Nozawa, H. Gailhanou, L. Raison, P. Panizza, H. Ushiki, E. Sellier, J.P. Delville, M.H. Delville, Smart control of monodisperse Stöber silica particles: effect of reactant addition rate on growth process, Langmuir 21 (2005) 1516–1523.
[44] V.K. LaMer, R.H. Denegar, Theory, production and mechanism of formation of monodispersed hydrosols, J. Am. Chem. Soc. 72 (1950) 4847–4854.
[45] F.B. Cottam, S. Krishnadasan, J.A. de Mello, C.J. de Mello, M. Shaffer, Accelerated synthesis of titanium oxide nanostructures using microfluidic chips, Lab Chip 7 (2007) 167–169.
[46] J.B. Edel, R. Fortt, J.C. deMello, A.J. deMello, Microfluidic routes to the controlled production of nanoparticles, Chem. Commun. 113 (2002) 6–1137.
[47] D. Shalom, R. Wootton, R.F. Winkle, B.F. Cottam, R. Vilar, A.J. de Mello, C.P. Wilde, Synthesis of thiol functionalized gold nanoparticles using a continuous flow microfluidic reactor, Mater. Lett. 6 (1) (2007) 1146–1150.
[48] Y. Song, C. Kumar, J. Hormes, Synthesis of palladium nanoparticles using a continuous flow polymeric micro reactor, J. Nanosci. Nanotechnol. 4 (2004) 788–793.
[49] W.B. Lee, C.H. Weng, F.Y. Cheng, C.S. Yeh, H.Y. Lei, G.B. Lee, Biomedical microdevices synthesis of iron oxide nanoparticles using a microfluidic system, Biomed. Microdevices 11 (2009) 161–171.
[50] A. Toyota, H. Nakamura, H. Ozono, K. Yamashita, M. Uehara, H. Maeda, Combinatorial synthesis of CdSe nanoparticles using microreactors, J. Phys. Chem. C 114 (2010) 7527–7534.